Journal of Orthopaedic Translation (2017) 8, 49—61

Available online at www.sciencedirect.com

ScienceDirect

journal homepage: http://ees.elsevier.com/jot

ORIGINAL ARTICLE

Bacterial inhibition potential of quaternised chitosan-coated VICRYL absorbable suture: An *in vitro* and *in vivo* study

Ying Yang, Sheng-Bing Yang, Yu-Gang Wang, Shu-Hong Zhang, Zhi-Feng Yu, Ting-Ting Tang*

Shanghai Key Laboratory of Orthopedic Implants, Department of Orthopedic Surgery, Shanghai Ninth People's Hospital, Shanghai Jiao Tong University, School of Medicine, Shanghai, People's Republic of China

Received 11 August 2016; received in revised form 5 October 2016; accepted 12 October 2016
Available online 11 November 2016

KEYWORDS
antibacterial sutures;
biocompatibility;
orthopaedic surgery;
quaternised chitosan;
surgical site infection

Summary *Background/Objective:* As a widely used absorbable suture with antibacterial property, triclosan- coated polyglactin suture (Vicryl Plus) has been extensively utilized to reduce the occurrence rate of surgical site infections (SSIs) in orthopaedic surgery. However, the potential toxicity and side-effects of triclosan raised increasing concerns about its biological safety. This study aimed to investigate the antimicrobial activity and biocompatibility of quaternised chitosan-coated Vicryl suture (HV) both *in vitro* and *in vivo*.
Methods: In this study, a modified chitosan derivate, (hydroxypropyltrimethyl ammonium chloride chitosan, HACC), was coated over the surface of the absorbable Vicryl suture. Two standard bacteria strains, *Staphylococcus epidermidis* (ATCC35984) and methicillin-resistant *Staphylococcus aureus* (ATCC43300), were selected to evaluate bacterial adhesion and biofilm formation on the sutures at 6, 24 and 48 h in vitro. Additionally, human skin-derived fibroblasts cells were used to test the cytocompatibility of the sutures. Furtherly, sutures contaminated with methicillin-resistant *S. aureus* were implanted subcutaneously in SD rats in order to confirm the *in vivo* antibacterial performance and biocompatibility.
Results: We found that HACC-coated Vicryl suture (HV) exhibited significant anti-bacterial effects on the two tested strains. The bacterial attachment and biofilm formation on the surface of the HV sutures were found to be comparable to that of Vicryl Plus sutures (VP). Moreover, all the four tested sutures presented good cytocompatibility with human skin-derived fibroblasts cells. Histology and immunohistochemistry results indicated that the infections and inflammations were significantly inhibited around the HV and VP sutures.

* Corresponding author. Shanghai Key Laboratory of Orthopedic Implants, Department of Orthopedic Surgery, Shanghai Ninth People's Hospital, Shanghai Jiao Tong University, School of Medicine, 639 Zhizaoju Road, Shanghai 200011, People's Republic of China.
E-mail address: ttt@sjtu.edu.cn (T.-T. Tang).

http://dx.doi.org/10.1016/j.jot.2016.10.001

Conclusion: In general, the present study demonstrated that the quaternised chitosan coating is a flexible and cost-effective alternative strategy to prevent the suture related surgical site infections in orthopaedic practices.

Introduction

Surgical site infections (SSIs) account for the most common complications postsurgery, which inevitably increases the prolonged hospitalisation, medical costs, and secondary patient morbidity [1,2]. Approximately 40% of all hospital-acquired infections are closely related to SSIs among surgical patients [3]. The incidence of infection involved in orthopaedic traumatic procedures has been estimated to be approximately 27% in civilians and 40% in war injuries, thus, infection serves as a major challenge and complication of orthopaedic trauma and reconstruction surgery [4]. Moreover, periprosthetic joint infection after total hip arthroplasty remains one of the most devastating complications [5]. As a foreign material to the surgical region, the implanted suture always functions as a nidus for infection under the condition of wound contamination, leading to recalcitrant and recurrent infections [6].

To reduce bacterial attachment to surgical sutures, triclosan-coated polyglactin sutures (Vicryl Plus, VP) with antibacterial potential were developed and have been widely used in the United States and Europe since 2003. Its efficacy in preventing SSIs has been extensively investigated and verified by various clinical cohort studies, randomised controlled trials, and meta-analysis, which consistently reach the conclusion that such an antibiotic-coated suture could effectively decrease the SSIs rates after surgery [7—11]. Triclosan, a broad-spectrum antibacterial agent, has been considered to interfere with bacterial lipid synthesis and consequently decrease bacterial colonisation of the suture material in both *in vitro* and *in vivo* studies [12,13]. Currently, the potential toxicity and side-effects of triclosan have raised increasing concerns about its biological safety. Several reports indicated that triclosan was physiologically harmful to the reproductive health in humans and animal models [14,15]. Triclosan has also been reported to promote *Staphylococcus aureus* nasal colonisation, resulting in relevant adverse effects on the environment and human health [16]. Metal ions with good antibacterial property, such as silver, have been used to modify the sutures [17,18]. However, cell and tissue compatibility have yet to be fully established. In addition, nanostructured sutures also showed desirable bacterial repellence performances, but their topography-based antibacterial property may not be suitable for combating contaminated SSIs [19]. Therefore, exploitation of alternative suture materials with excellent antibacterial activity and good biocompatibility is of major scientific and clinical significance.

It has been found that the antimicrobial activity and biocompatibility of hydroxypropyltrimethylammonium chloride chitosan (HACC), a water-soluble chitosan derivative, could be adjusted by varying the degree of substitution (DS) of quaternary ammonium [20]. Our previous studies indicated that HACC exhibited excellent antibacterial potential and good biocompatibility both *in vitro* and *in vivo* [21—24]. HACC exhibited a broad spectrum of antibacterial activity because of the electrostatic interaction between the positively charged quaternary ammonium groups of HACC and the negatively charged phosphoryl groups of the phospholipid components of bacterial membranes, which affected the cytoplasmic membrane integrity and eventually led to cell death [25,26]. Thus, such a physically antibacterial effect of HACC on microbes may not induce antibiotic resistance and enzymatic dysfunction, as previously reported to be caused by triclosan [14—16]. In the present study, we investigated the antimicrobial activity and biocompatibility of this innovative HACC-coated Vicryl (HV) suture both *in vitro* and *in vivo*. In addition, absorbable Vicryl (V), VP, and gentamicin-coated Vicryl (GV) sutures were also studied and compared. We hypothesised that the HACC coating over the suture could significantly improve the antibacterial activity with good biocompatibility, which may pave the way for developing new cationic antimicrobial agent-coated sutures in future orthopaedic surgery.

Materials and methods

Materials

Gentamicin sulphate salt [molecular weight (MW) = 547.62 g/moL], triclosan (MW = 289.50 g/moL), glycidyl trimethylammonium chloride (MW = 151.63 g/moL), and type I collagen from calf skin were purchased from Sigma-Aldrich, Ltd. (St. Louis, MO, USA). Chitosan (MW = 50,000 g/moL) with 87% N-deacetylation was purchased from Zhejiang Yuhuan Ocean Biochemistry Co., Ltd., Yuhuan, Zhejiang, China. HACC (MW = 200,000 g/moL) with a 26% DS of quaternary ammonium was prepared by combining chitosan and GTMAC, as previously reported [20,22]. All other chemical reagents were of analytical grade and were purchased commercially.

Preparation of gentamicin and HACC-coated sutures

VP antibacterial absorbable sutures and V absorbable sutures were purchased from Ethicon Ltd. (Somerville, NJ, USA). Firstly, type I collagen was dissolved in 5mM acetic acid at a concentration of 0.5 mg/mL according to the provided manufacture's protocols. Subsequently, gentamicin or HACC with a mass concentration of 0.2 wt% was

dissolved in 50 mL of prepared collagen solutions, and sonicated in an ultrasonic bath at 150 W (B3500S-MT, Branson, Shanghai, China operating at a frequency of 50 Hz for 5 minutes to obtain the uniformly dissolved solutions. Then, Vicryl absorbable sutures were immersed overnight in the solutions to form the antibacterial agent-coated sutures as described in a previous report [27]. After the adsorption of collagen, the sutures were dried at room temperature for 24 hours. In each group, the same suture size was used for the *in vitro* (2-0) and *in vivo* (4-0) experiments, and all the tested sutures were cut into 2.5 cm in length for the *in vitro* assay (except for the sutures with lengths of 10 cm used for the *in vitro* drug release measurement). All prepared GV and HV sutures were sterilised by 25 kGy of ^{60}Co irradiation before the biologic experiments were conducted.

Surface characterisation

The elemental distribution of the sutures was determined using energy-dispersive X-ray spectroscopy (JEOL JSM-6310LV, JEOL Ltd., Tokyo, Japan). Meanwhile, the surface morphologies of the four sutures were examined using a scanning electron microscope (SEM, HITACHI SU8220, Tokyo, Japan) at an electron acceleration voltage of 3.0 kV.

Characterisation of drug release from sutures

The release kinetics of the gentamicin and HACC from the sutures were determined as described in our previous studies [28,29]. Five sutures coated with gentamicin (GV) or HACC (HV) were each individually immersed in 2 mL of phosphate-buffered saline (PBS) at 37°C and agitated at 100 rpm. V immersed in 2 mL of PBS served as blank controls. All drug-coated sutures were taken after specific intervals to confirm the release kinetics with a periodic collection for up to 144 hours. The solution was replaced with 2 mL of fresh PBS every time sutures were collected. The colorimetric evaluation was used to determine the released gentamicin content [30]. In brief, the collected gentamicin solution, isopropanol, and o-phthaldialdehyde reagent (560 mL of sodium borate solution added with 2.5 g o-phthaldialdehyde, 62.5 mL of methanol, and 3 mL of 2-mercaptoethanol) were adequately mixed and incubated at 37°C for 30 minutes. Then, the absorbance of these products was determined at 332 nm using a Synergy HT microplate reader (Bio-Tek Instruments Ltd., Winooski, VT, USA).

In addition, the released HACC content was confirmed using the anthrone sulphuric acid reaction [31]. Briefly, 50 μL of solution taken from no drug-loaded sutures, 50 μL of solution collected from HACC-coated sutures, and 50 μL of standard glucose solution with gradient concentrations were individually placed into 96-well plates (Costar; Corning Incorporated, New York, NY, USA), and then gently vortexed (Vortex-Genie 2; Scientific Industries, New York, NY, USA) and incubated at 4°C for 15 minutes. Subsequently, 100 μL of freshly prepared anthrone solution was added into each well. Then, the plate was thoroughly vortexed and incubated in a water bath at 92°C for 3 minutes. The absorbance of these products was determined at 630 nm after 5 minutes cooling at room temperature. A standard curve with known concentration of gentamicin ($y = 0.003x + 0.026$, $R^2 = 0.986$, x and y denote the gentamicin concentration and absorbance, respectively) or glucose ($y = 0.002x + 0.057$, $R^2 = 0.982$, x and y denote the HACC concentration and absorbance, respectively) standard samples was used to determine the unknown gentamicin or HACC concentrations (μg/mL), respectively. After a thorough degradation in type I collagenase water solution (1 mg/mL, Sigma-Aldrich) for 48 hours at 37°C under an agitation at 100 rpm, the total drug loading amounts of GV and HV sutures were calculated according to the methods mentioned above.

Preparation and characterisation of bacteria

Staphylococcus epidermidis (ATCC35984) and methicillin-resistant *S. aureus* (MRSA, ATCC43300) were purchased from the American Type Culture Collection (Manassas, VA, USA). The cells were suspended in Mueller-Hinton Broth (MHB, Solarbio, Beijing, China) at 1×10^8 colony-forming units (CFUs)/mL after overnight tryptic soy broth culture, according to a McFarland standard protocol (Beijing Zhecheng Science and Technology Co., Ltd., Beijing, China). The minimum inhibition concentrations (MICs) of triclosan, gentamicin, and HACC with a 26% DS of quaternary ammonium against these two tested strains were determined according to a previously reported microtiter broth dilution method [32]. In brief, 100 μL of bacteria suspension in MHB with a density of 1.0×10^6 CFUs/mL was inoculated into 96-well plates (Costar in the presence of triclosan, gentamicin, and HACC with a 26% DS at different final concentrations (0 μg/mL, 1 μg/mL, 2 μg/mL, 4 μg/mL, 8 μg/mL, 16 μg/mL, 32 μg/mL, 64 μg/mL, 128 μg/mL, 256 μg/mL, 512 μg/mL, and 1024 μg/mL). The inoculated microplates were incubated at 37°C for 24 hours before further analysis.

In vitro anti-bacterial performance

Zone of inhibition assay

The zone of inhibition assay was used to compare the antimicrobial efficacy against the two tested strains for these sutures [33]. In brief, bacterial suspension at a concentration of 1×10^8 CFUs/mL in MHB medium was inoculated onto the 10 cm tryptic soy agar (TSA) plate to obtain a uniform bacterial overlay, then the prepared sutures were placed on the bacterial overlay and gently pressed in. Inhibition zones of all the tested sutures were photographed and calculated after 24 hours incubation at 37°C.

Bacterial adhesion and biofilm formation assay

Bacterial adhesion on the sutures was determined using the spread plate method [34]. A volume of 1 mL of bacterial suspensions at an amount of 1×10^6 CFUs/mL in MHB medium was added into wells containing V, VP, GV, and HV sutures, and these were then incubated at 37°C for 4 hours. The adherent bacteria on the sutures were dislodged by ultrasonication in the ultrasonic bath operating at a frequency of 50 Hz for 5 minutes. The solutions collected after ultrasonication were then serially diluted 10-fold and were plated in triplicate onto TSA. They were then transferred into an incubator with a temperature of 37°C and incubated for 24

hours. The number of colonies on the TSA was counted, and the ultimate number of CFUs on the suture was the number of colonies multiplied by the dilution ratio. The CFUs of each group were normalised to the counts from the V sutures.

The tissue culture plate method was used to detect biofilm formation [35]. After 24 hours and 48 hours of incubation, the sutures were dried at 60°C for 1 hour. Then, the biofilms on the sutures were stained with 500 μL of a 0.1% (wt/vol) aqueous solution of crystal violet (CV; Sigma-Aldrich) at room temperature for 10 minutes. The sutures were then dried at 37°C for 2 hours. Then, biofilm formation was quantified by solubilisation of the CV stain in 200 μL of 30% (wt/vol) glacial acetic acid for 10 minutes with shaking at 300 rpm. The CV concentration was determined at 492 nm. The mean absorbance obtained from the medium control well was subtracted from the test absorbance values.

Confocal laser scanning microscopy and SEM observation

MRSA (ATCC43300) was selected for the observation of confocal laser scanning microscopy (CLSM) and SEM. After 6 hours and 24 hours of co-culture, the sutures were gently washed three times with PBS, and then stained with 500 μL of combination dye (LIVE/DEAD BacLight viability kits, L7012; Thermo Fisher Scientific, Waltham, MA, USA) and were visualised using CLSM (Leica TCS SP8, Leica Microsystems, Wetzlar, Germany). Viable bacteria with intact cell membranes appear fluorescent green, whereas nonviable bacteria with damaged cell membranes appear fluorescent red. The three-dimensional images were acquired from random suture positions. The adherent bacteria and biofilm on the sutures were then dehydrated through a series of graded ethanol solutions (30%, 50%, 70%, 80%, 90%, and 100%) for 10 minutes each after fixation in 2.5% glutaraldehyde solution for 2 hours at 4°C. The sutures were subsequently examined using SEM after critical-point drying and coating by gold sputter.

In vitro cytocompatibility

Human skin-derived fibroblasts, isolated and expanded as previously described [36], were selected to evaluate the cytocompatibility of these sutures *in vitro*. A cell counting kit-8 (CCK-8) assay was used to analyse the cell proliferation at 6 hours, 24 hours, 72 hours, and 120 hours according to the previously reported protocols [37]. In brief, cell suspension was seeded into a 24-well plate containing various sutures at a density of $3.0 \times 10^4/cm^2$, with α-MEM (Modified Eagle's Medium) medium as a blank control. The sutures were removed, and 50 μL of CCK-8 solution (Dojindo Molecular Technologies Inc., Kumamoto, Japan) was added to the wells without sutures at each time point. The mixed solutions were incubated for 3 hours, and then read at 450 nm with 620 nm as the reference wavelength. The mean absorbance value (optical density, OD) obtained from the blank control was subtracted from the ODs of the tested groups.

In addition, the cell viability was further analysed using a Live/Dead Cell kit (ab115347, Abcam, Cambridge, UK) through the evaluation of flow cytometry. The cell seeding procedures were similar to those of the cell proliferation, except that the cell seeding density was $1.5 \times 10^5/cm^2$ in a six-well plate. After a 24-hour co-culture, cells were trypsinised and collected, staining with 200 μL of combination dye for 10 minutes according to the manufacturer's protocol. All samples were run on a BD LSRFortessa (BD Biosciences, San Jose, CA, USA) and data were analysed using FlowJo software (TreeStar, Ashland, OR, USA).

Anti-infective potential and biocompatibility *in vivo*

Animal experiment

We here established a subcutaneous implantation model to evaluate the anti-infection performances of the sutures *in vivo*. All experimental procedures were approved and performed in accordance with the guidelines of the Animal Ethics Committee of Shanghai Ninth People's Hospital. In brief, 24 6-week-old Sprague-Dawley male rats weighing approximately 300 g were assigned randomly to four independent groups: V, VP, GV, and HV. The rats were initially anaesthetised using an intraperitoneal injection of 1% pentobarbital sodium (100 mg/kg body wt) and both of the lateral thighs were shaved and cleaned with 2% iodine prior to the procedure. An approximately 3 cm longitudinal skin incision was made over the lateral thighs and reached the musculoaponeurotic layer, then the superficial muscle was incised at a length of approximately 2.5 cm. Prior to the suture of the incised superficial muscle in the left thigh, these tested sutures were incubated with the prepared ATCC43300 suspensions (1×10^6 CFUs/mL in PBS) for 5 minutes. Meanwhile, sutures without bacteria inoculation were implanted in the right thigh to evaluate the *in vivo* biocompatibility. Then, the skin closure was performed using 4-0 Mersilk nonabsorbable sutures (Ethicon). The rats were housed in ventilated rooms and allowed to eat and drink *ad libitum* after surgery. The animals were sacrificed 21 days after implantation. No antibiotics were administered, and no mortality occurred during the experiment. All animal operations were performed by the same person under the same experimental condition.

Histopathological evaluation

The implanted sutures and the peri-implant tissues in each group were harvested at 21 days after implantation, and then immersed in 4% neutral-buffered formaldehyde for 48 hours. The collected specimens were then embedded into paraffin. The embedded specimens were cut into sections parallel to the cross-section of the sutures and prepared at a thickness of 5 μm (EXAKT-400 grinding equipment, SLEE Medical, Mainz, Germany). Haematoxylin and eosin and Giemsa staining were used to assess morphology and bacterial contamination, respectively. Meanwhile, immunohistochemical staining was also used to observe the inflammatory cells (lymphocyte and macrophage) surrounding the sutures according to the previous protocol [38]. In brief, prepared slices were incubated overnight at 4°C with anti-CD3 antibody (1:100, ab16669, Abcam, Cambridge, UK) or anti-CD68 antibody (1:400, ab955, Abcam) after deparaffinisation, rehydration with descending concentrations of ethanol, quenching of endogenous peroxidase, and blocking with 3% bovine serum albumin. Then, the sections were visualised using diaminobenzidine (DakoCytomation, Glostrup, Denmark) containing biotinylated anti-rat IgG secondary antibody. The histological images were captured on a Leica AF6000 (Leica Microsystems, Wetzlar, Germany).

Statistical analysis

All data are expressed as the mean ± standard deviation. All *in vitro* experiments were repeated three times. One-way analysis of variance (ANOVA), the least significant difference test and nonparametric test (Mann-Whitney *U* test) were used to determine the level of significance; $p < 0.05$ was defined as statistically significant, and $p < 0.01$ was considered highly statistically significant. All statistical analyses of the data were performed using SPSS software (v19.0, IBM Corp, Armonk, NY, USA).

Results

Morphological characterisation and drug releasing

The elemental distributions of C, O, and N in the sutures obtained by Energy Dispersive Spectroscopy (EDS) are shown in Figure 1A, and the images indicate that elemental

Table 1 The initial and total releasing of drugs in 144 hours.

Sutures	Loaded drugs	Total drug-loaded (μg[a]/one suture)	Initial release (μg[b])	Total release (μg)
GV	Gentamicin	318.38	92.90	117.16
HV	HACC	349.48	143.45*	175.73*

* $p < 0.05$ compared with GV sutures ($n = 5$).
GV = gentamicin-coated Vicryl suture; HV = hydroxypropyltrimethylammonium chloride chitosan (HACC)-coated Vicryl suture.
[a] The total drug loading amount in the sutures was measured after a thorough degradation in type I collagenase water solution.
[b] The amount of drug released in the initial burst release period before the drug release rate became nearly constant.

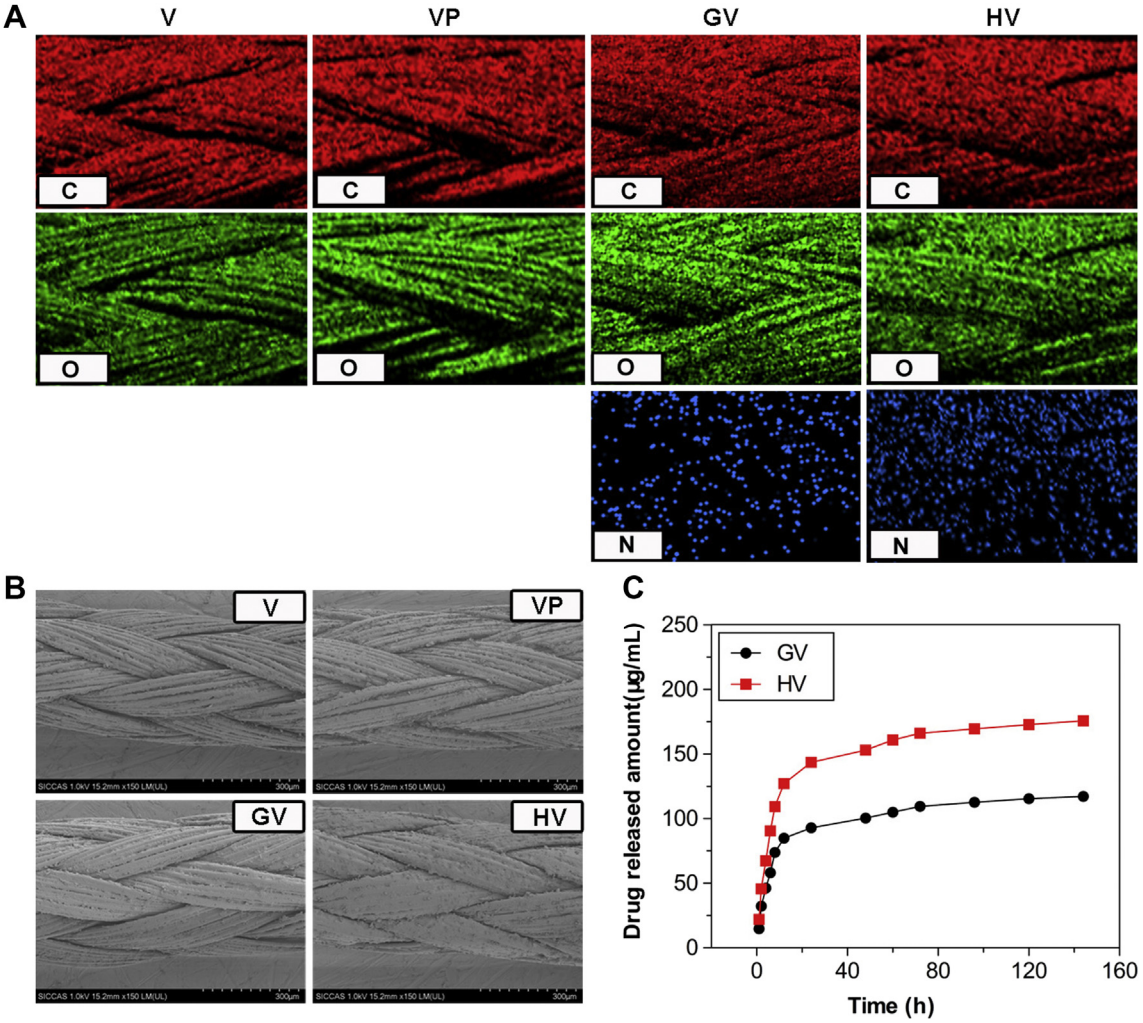

Figure 1 Surface and drug releasing characterisation of absorbable Vicryl suture (V), Vicryl Plus (VP) suture, gentamicin-coated Vicryl (GV) suture and hydroxypropyltrimethylammonium chloride chitosan (HACC)-coated Vicryl (HV) suture. (A) Energy Dispersive Spectroscopy (EDS) elemental mapping of a randomly selected area showing the distributions of C, O, and N elements; (B) representative scanning electron microscopy (SEM) images; (C) cumulative drug release profiles from GV (gentamicin) and HV (HACC) sutures ($n = 5$), expressed in μg/mL.

Table 2 The minimum inhibiting concentrations of the two tested strains.

Compounds	MICs (μg/mL)	
	ATCC 35984	ATCC 43300
Triclosan	32	64
Gentamicin	16	512
HACC (26%DS[a])	32	64

HACC = hydroxypropyltrimethylammonium chloride chitosan; MIC = minimum inhibition concentration.
[a] Degree of substitution of quaternary ammonium.

N derived from gentamicin and HACC existed in GV and HV sutures exclusively. The morphology of the sutures was observed using SEM. As demonstrated in Figure 1B, the gaps between the threads of the sutures were evidently covered by the coated drugs incorporated in collagen. These results could be evidence of successfully coated gentamicin and HACC over the surfaces of the sutures.

As shown in Figure 1C, there is higher sustained drug release from HV than from GV ($p < 0.05$). The majority of the gentamicin or HACC was released from the sutures after approximately 24 hours. We found that drugs released from the sutures could be divided into two parts: initial burst release and relatively slow release. The amount of gentamicin or HACC released from the sutures remained nearly constant after a high initial burst release. As demonstrated in Table 1, the total drug loading of gentamicin and HACC from sutures was 318.38 μg and 349.48 μg, respectively ($p > 0.05$). The initial release of gentamicin and HACC from sutures was 92.90 μg and 143.45 μg, respectively, ($p < 0.05$). In addition, the results indicated that approximately 60% and 50% drugs were retained in the GV and HV sutures after 144 hours releasing, respectively ($p < 0.05$).

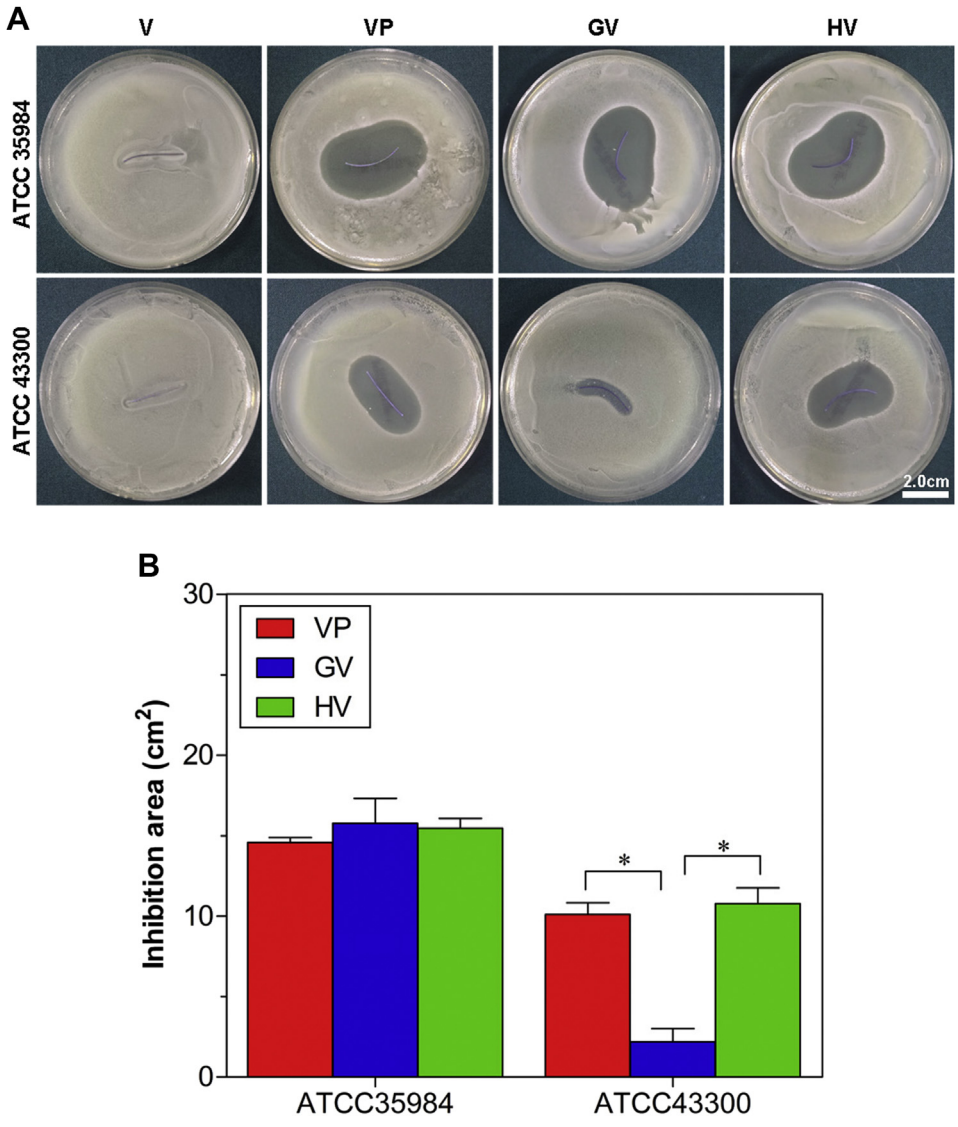

Figure 2 Comparison of the antibacterial efficacy of various sutures against the two strains after 24 hours incubation. (A) Photographed inhibition zone affected by different sutures; (B) quantification of the inhibition zone. * $p < 0.01$ compared with GV ($n = 5$). GV = gentamicin-coated Vicryl suture; HV = hydroxypropyltrimethylammonium chloride chitosan (HACC)-coated Vicryl suture; V = absorbable Vicryl suture; VP = Vicryl Plus suture.

Antibacterial properties of the drugs contained in sutures

The phenotype classification and biofilm-forming capacity were confirmed previously [22]. The MICs of triclosan, gentamicin, and HACC with a 26% DS were 32 μg/mL, 16 μg/mL, and 32 μg/mL against S. *epidermidis* (ATCC35984), respectively (Table 2). Alternatively, the MICs of triclosan, gentamicin, and HACC with a 26% DS were 64 μg/mL, 512 μg/mL, and 64 μg/mL against MRSA (ATCC43300), respectively. These results indicated that triclosan and HACC with a 26% DS showed significant antibacterial capabilities on the antibiotic-resistant strain (ATCC43300), which is difficult to be inhibited by gentamicin.

Antibacterial potential and cytocompatibility *in vitro*

Zone of inhibition

In order to compare the antimicrobial efficacy *in vitro*, we photographed and calculated the inhibition zones in various groups after 24 hours incubation. As shown in Figure 2, the areas of the inhibition zone of the three antibiotic-coated sutures (VP, GV, and HV) exhibited no significant differences for the strain ATCC35984 ($p > 0.05$), whereas the inhibition zone of the GV against the strain ATCC43300 was evidently lesser than VP and HV ($p < 0.01$).

Inhibition of bacterial adherence and biofilm formation

The surviving number of the two strains on different sutures at 6 hours was quantitatively determined by the spreading plate method, as shown in Figures 3A and 3B. The numbers of viable bacteria on the surface of V were significantly higher than those on the other three sutures ($p < 0.01$), and no differences were observed among the VP, GV, and HV for the strain ATCC35984 ($p > 0.05$). However, the numbers of viable bacteria of methicillin-resistant ATCC43300 on the surface of GV were found to be significantly higher than those on the VP and HV sutures ($p < 0.01$). Considering log-reduction with respect to V, ATCC35984 on VP, GV, and HV sutures were reduced 1.29-log, 1.65-log, and 1.37-log at 6 hours, respectively, and ATCC43300 on VP, GV, and HV sutures were reduced 0.82-log, 0.15-log, and 0.78-log, respectively.

The biofilm-formation evaluation using the tissue culture plate method is shown in Figures 3C and 3D. The OD_{492} values of the VP, GV, and HV groups for ATCC35984 were significantly lower than those of the V group at 24 hours and

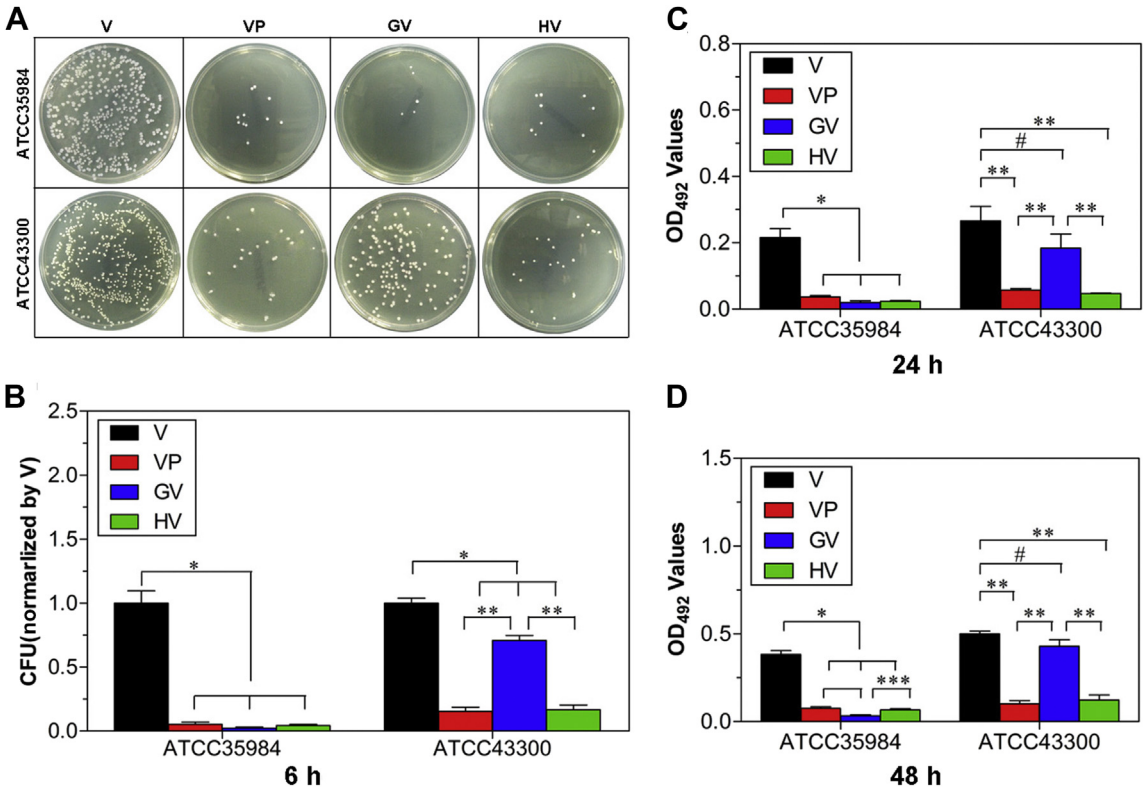

Figure 3 Bacterial adhesion and biofilm formation evaluation. (A) Representative images of adherent bacteria on the surfaces of the four sutures after 6 hours of incubation. (B) The number of viable bacteria on VP, GV, and HV sutures normalised to the counts from V sutures for the two tested strains at 6 hours, as measured using the spread plate method. (C), (D) Biofilm formation of the two tested strains on the surfaces of various sutures at 24 hours and 48 hours, respectively, as evaluated by the tissue culture plate method. * $p < 0.01$ compared with the other three sutures ($n = 5$). ** $p < 0.01$ compared with VP and HV sutures ($n = 5$). *** $p < 0.05$ compared with HV suture ($n = 5$). $^{\#}p < 0.05$ compared with GV suture ($n = 5$). GV = gentamicin-coated Vicryl suture; HV = hydroxypropyltrimethylammonium chloride chitosan (HACC)-coated Vicryl suture; V = absorbable Vicryl suture; VP = Vicryl Plus suture.

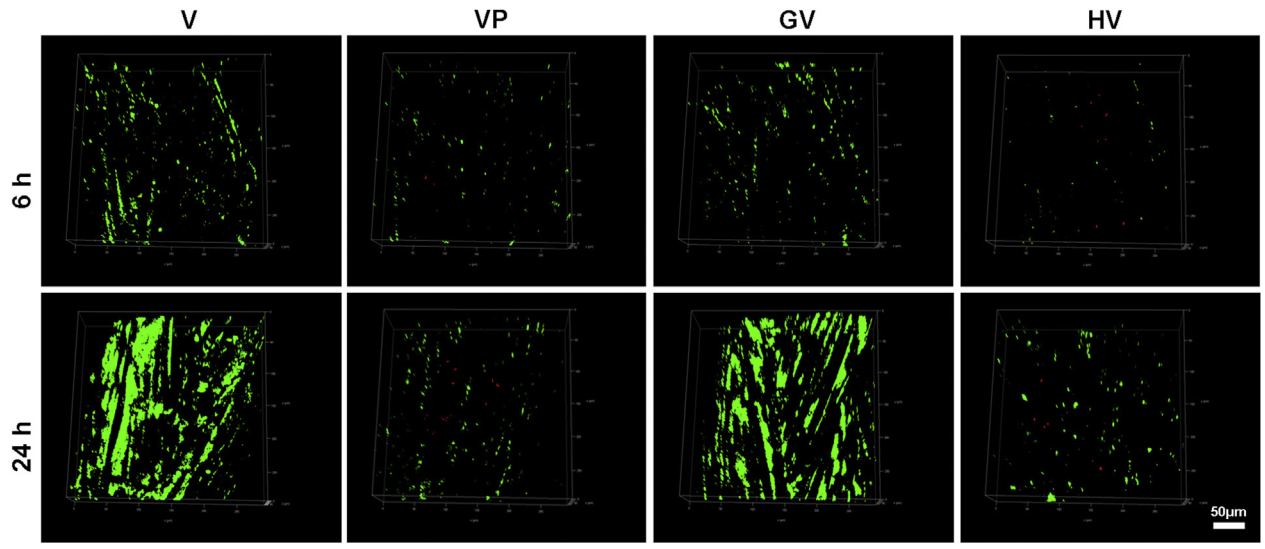

Figure 4 Confocal laser scanning microscopy (CLSM) observation of bacterial viability and biofilm formation of ATCC43300 on the surfaces of V, VP, GV, and HV sutures at 6 hours and 24 hours after the sutures were stained with the BacLight Live/Dead stain. Bacteria were stained with green fluorescent SYTO 9 and red fluorescent propidium iodide, which denoted live and dead cells, respectively. GV = gentamicin-coated Vicryl suture; HV = hydroxypropyltrimethylammonium chloride chitosan (HACC)-coated Vicryl suture; V = absorbable Vicryl suture; VP = Vicryl Plus suture.

48 hours ($p < 0.01$). In addition, the OD_{492} values of the GV group for ATCC35984 were also significantly lower than HV at 48 hours ($p < 0.05$). For the methicillin-resistant strain ATCC43300, the OD_{492} values of the VP and HV groups were significantly lower than those of the V and GV groups at the two time points ($p < 0.01$). The OD_{492} values of the GV group were significantly lower than those of the V at the two time points ($p < 0.05$). Our results demonstrated that

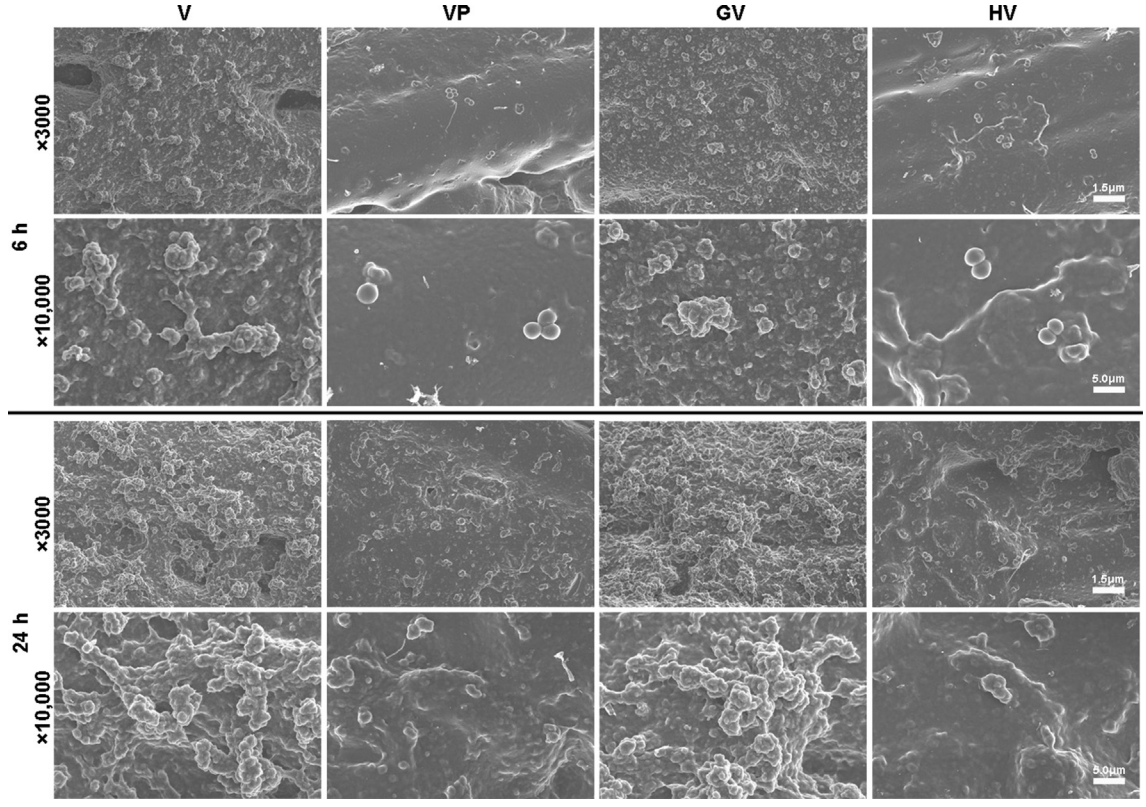

Figure 5 Scanning electron microscopy (SEM) observation of bacterial adhesion and biofilm formation of ATCC43300 on the surfaces of V, VP, GV, and HV sutures at 6 hours and 24 hours. GV = gentamicin-coated Vicryl suture; HV = hydroxypropyltrimethylammonium chloride chitosan (HACC)-coated Vicryl suture; V = absorbable Vicryl suture; VP = Vicryl Plus suture.

all three antibiotic-coated sutures displayed obvious antibacterial effects on the ATCC35984, but discrepant effects on the ATCC43300.

CLSM and SEM observation

Bacterial adhesion and biofilm formation of ATCC43300 on the surfaces of various sutures at 6 hours and 24 hours were observed using CLSM and SEM. As shown in Figure 4, live bacteria appeared fluoresced green, and dead bacteria fluoresced red. At 6 hours, considerably less green fluorescence and scattered red fluorescence could be found on the VP and HV sutures, which indicated a significant decreased level of adherent surviving bacteria on the VP and HV sutures. An extraordinarily dense green fluorescence, indicating biofilm formation, was detected on the V and GV sutures at 24 hours. Conversely, a sparse red and green fluorescence, indicating dead colonies and no biofilm formation, was observed on the VP and HV sutures. Meanwhile, the SEM observations further supported the CLSM results as shown in Figure 5.

In vitro cytocompatibility evaluation

Cell proliferation measured using the CCK-8 assay was similar in all four groups during the 120 hours co-culture period ($p > 0.05$) (Figures 6A and 6B). Additionally, cells exhibited good viability in all four groups according to the results of flow cytometry (Figures 6D and 6D). Therefore, our results disclosed the good cytocompatibility in these groups *in vitro*.

Histopathological evaluation

The morphological changes and bacterial residues on the transverse slices are evaluated by haematoxylin and eosin

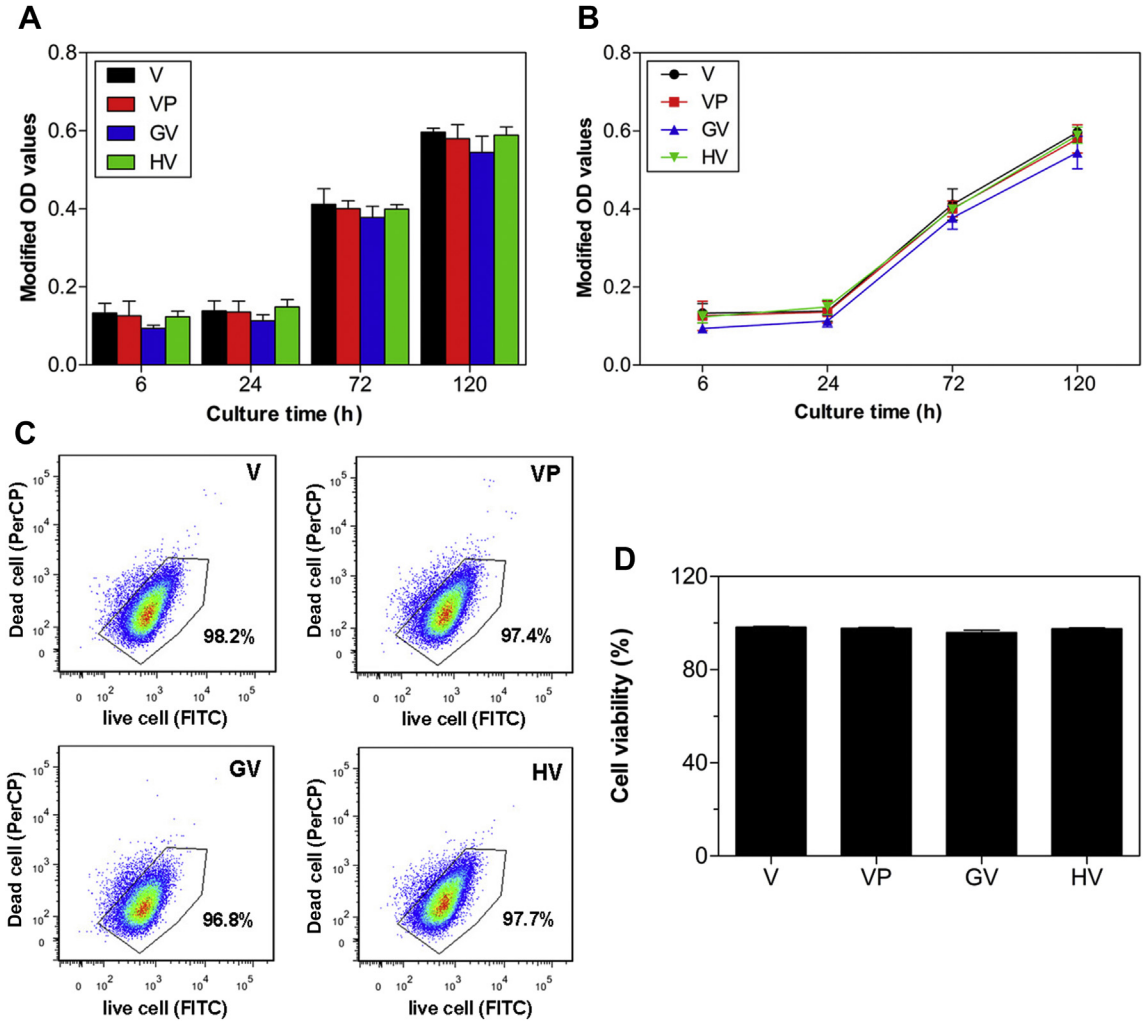

Figure 6 *In vitro* cytocompatibility of various sutures co-cultured with human fibroblasts (hFBs) at 6 hours, 24 hours, 72 hours, and 120 hours. (A), (B) Cell proliferation and tendency measured using the cell counting kit-8 assay. (C) Cell viability evaluated by the Live/Dead assay after 24 hours incubation using flow cytometry. Live cells are on the x-axis and dead cells are on the y-axis. The black polygon gate identifies live cells and the number indicates the percent of live cells. (D) Quantification of the ratio of live cells in various sutures after a 24-hour co-culture. FITC = fluorescein isothiocyanate; GV = gentamicin-coated Vicryl suture; HV = hydroxypropyltrimethylammonium chloride chitosan (HACC)-coated Vicryl suture; V = absorbable Vicryl suture; VP = Vicryl Plus suture.

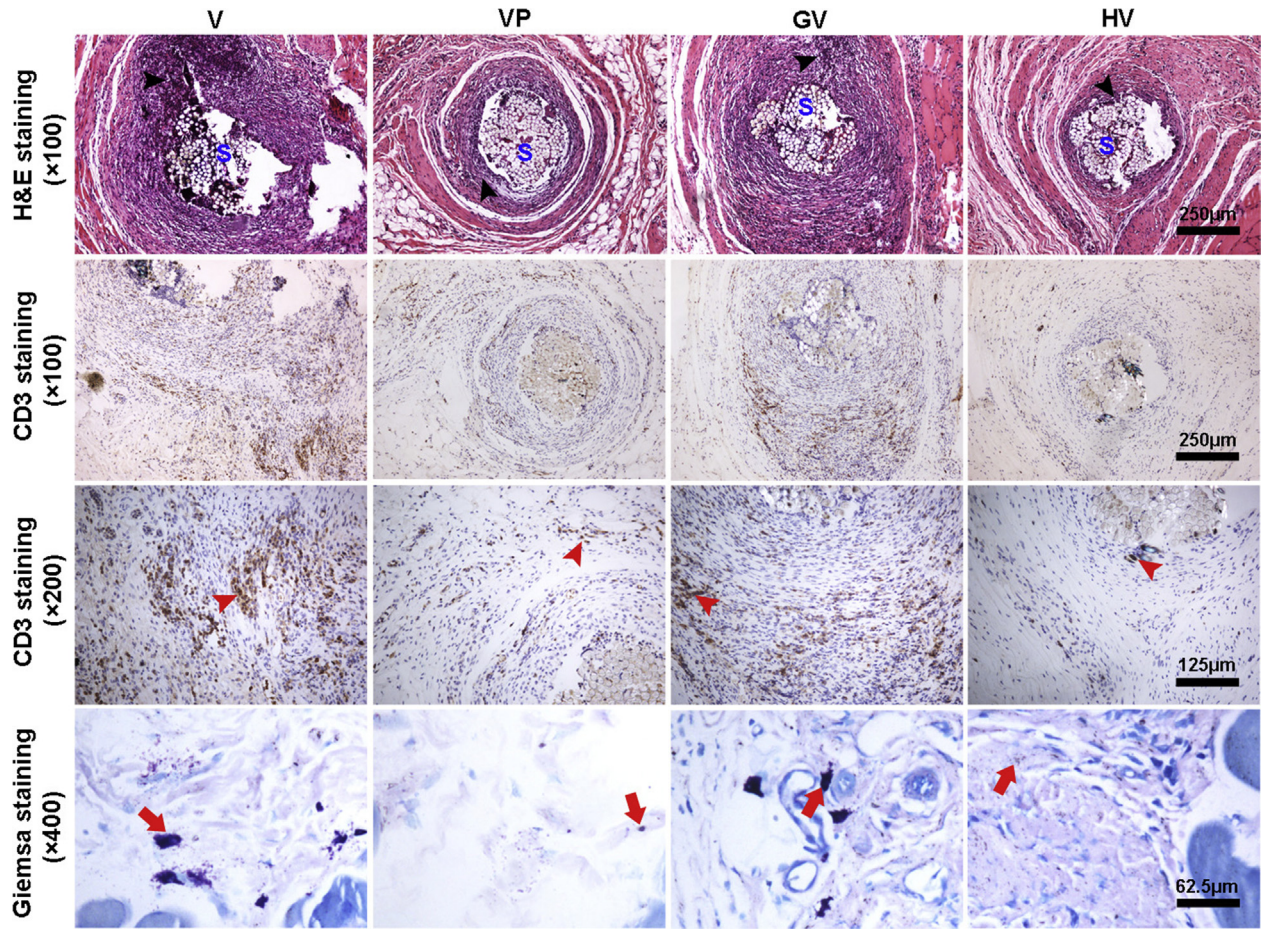

Figure 7 Histological evaluations of contaminated sutures with surrounding soft tissues obtained at 21 days after implantation. Immunohistochemical staining (CD3) was used to confirm the lymphocyte infiltration. Haematoxylin and eosin (H&E) and Giemsa staining were used to assess morphology and bacterial contamination, respectively. The black arrowheads indicate fibroplasia and inflammatory cell infiltration. The red arrowheads indicate lymphocyte infiltration and the red arrows indicate residual bacteria. GV = gentamicin-coated Vicryl suture; HV = hydroxypropyltrimethylammonium chloride chitosan (HACC)-coated Vicryl suture; S = sutures; V = absorbable Vicryl suture; VP = Vicryl Plus suture.

and Giemsa staining, respectively. Meanwhile, the leukomonocyte and macrophage infiltration is confirmed by immunohistochemical staining. As demonstrated in Figure 7, typical signs of soft-tissue infection around the sutures as manifested by the development of local necrosis, fibroplasia, and inflammatory cells infiltration, were found in the V and GV groups, and lots of bacteria are observed in the area around the sutures as manifested in the Giemsa slices at high magnification. In contrast, histological slices from the VP and HV groups exhibited small necrosis formation and significantly reduced inflammatory reaction, and the number of bacteria colonised around the sutures reduced dramatically. These results indicate that the VP and HV groups presented effective anti-infection performances.

Meanwhile, we further investigated the *in vivo* biocompatibility of these sutures. As shown in Figure 8, there was slight inflammatory reaction observed in all groups, and the macrophage infiltration was not obvious, which was consistent with *in vitro* cytocompatibility results.

Discussion

Implanted sutures may potentiate postoperative SSIs in the presence of wound contamination, since it lowers the inoculation amount required for infection in a clean surgical site [6,39]. The overall risk of SSIs following hip fracture surgery has been reported to be 4.97%, with approximately 30% cases among them representing deep infection [40]. Furthermore, the cost of treating a patient with SSIs has been counted to be £31,164, rising to £38,464 if the pathogenic bacteria is MRSA [41]. Routine antibiotic prophylaxis produced limited effects on decreasing the rate of SSIs in open reduction and internal fixation, especially under the contamination of drug-resistant strains [42]. All suture surfaces, regardless of structural configuration, can provide a hospitable environment for bacterial attachment [6]. Therefore, preventing bacterial adherence and biofilm formation on the surface of the implanted sutures would appear to be a favourable strategy for the risk reduction of SSIs. In this study, an innovative approach to solving these intractable challenges was

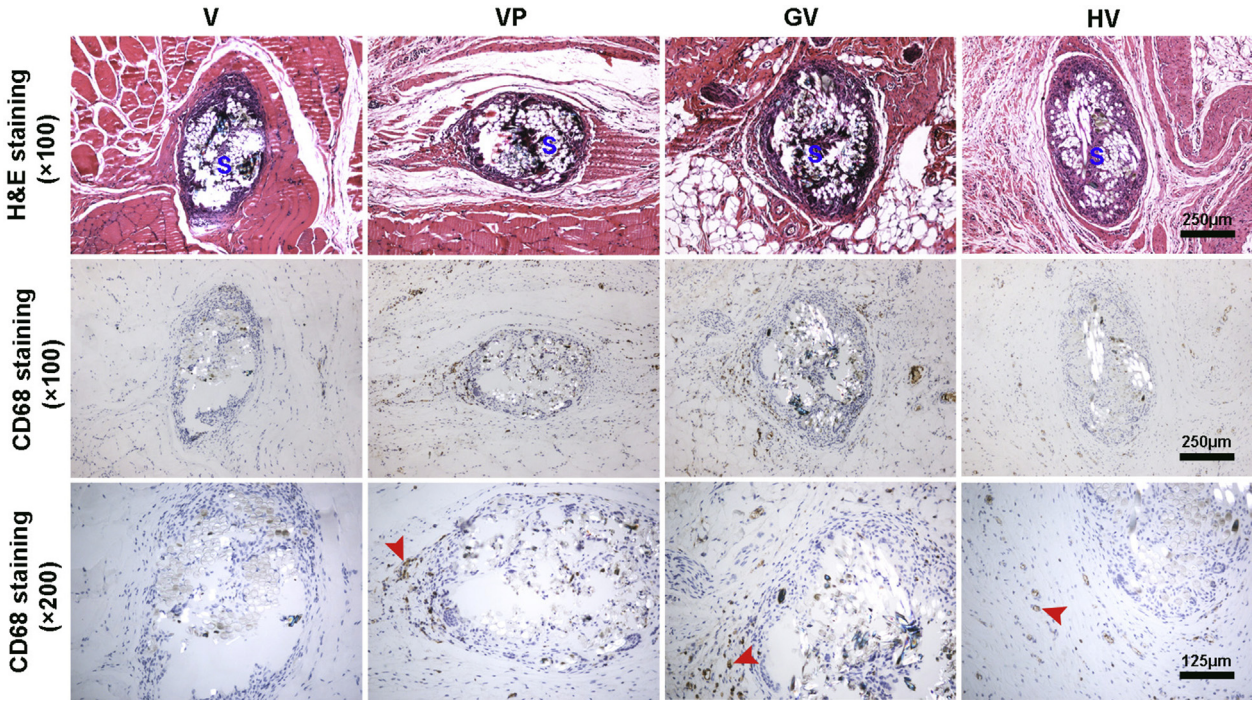

Figure 8 Histological evaluations of noncontaminated sutures with surrounding soft tissues. Haematoxylin and eosin (H&E) and immunohistochemical staining (CD68) were used to observe the morphology and macrophage infiltration, respectively. The red arrowheads indicate macrophage infiltration. GV = gentamicin-coated Vicryl suture; HV = hydroxypropyltrimethylammonium chloride chitosan (HACC)-coated Vicryl suture; S = sutures; V = absorbable Vicryl suture; VP = Vicryl Plus suture.

developed by coating HACC to the absorbable Vicryl suture.

The initial adherence of microbes to biomaterial surfaces is considered to be the key step for the pathogenesis of foreign body infections, and bacterial adhesion from 4–6 hours after implantation has been shown to be critical to biofilm formation [43]. *S. epidermidis* and MRSA, which are two common bacterial strains recovered from infected and noninfected patients according to a previous investigation [6], were selected to test the antimicrobial performances of the four different sutures. We concluded that gentamicin and HACC were successfully coated over the surfaces of the sutures according to the results of the morphological and elemental characterisation analysed above, which laid the foundation for the proceeding of the *in vitro* and *in vivo* antibacterial evaluations. In addition, we examined the drug releasing characteristics of sutures GV and HV, indicating that the initial drug release time of GV and HV was extended to approximately 24 hours. The total amounts of gentamicin and HACC released from the sutures were 117.16 μg and 175.73 μg, respectively, which were all above the MICs of *S. epidermidis* (ATCC35984), as analysed in Table 2. However, the total released gentamicin is insufficient to inhibit the adhesion and biofilm formation of MRSA (ATCC43300). Although nearly half of HACC was not released and retained in HV sutures, we may conclude that the released HACC is sufficient to produce desirable antibacterial performances.

Even though the antimicrobial coating prevents the accumulation of microbes on medical materials to some degree, it is very difficult to eliminate or kill bacteria that adhered to suture material once a biofilm has formed and matured [44]. The HACC-coated sutures exhibited parallel antibacterial activity, including significantly inhibited bacterial adherence and biofilm formation compared with triclosan-coated sutures. However, the gentamicin-coated sutures demonstrated limited antimicrobial capability against antibiotic resistant strains due to relatively high MICs. Meanwhile, all four different sutures displayed good biocompatibility both *in vitro* and *in vivo*. Although the short-term biocompatibility of the triclosan-coated suture was shown in our study, its potential adverse effects have been reported in previous studies [14–16]. Moreover, we have roughly estimated the fabrication cost of these antibacterial sutures according to the referred price of commercially purchased triclosan, gentamicin, and chitosan, indicating that per gram production cost of HACC was approximately 1/1000 and 1/50 of triclosan and gentamicin involved in the manufacture of antimicrobial agent-loaded sutures, respectively. Thus, we conclude that HACC may be a new and effective candidate for the fabrication of antibacterial sutures in the future, which is supposed to demonstrate good anti-infection potential, reduced side-effects, and significantly alleviated medical expenses.

Although the bacterial residues found in the Giemsa slices of the VP and HV groups were significantly more decreased than those in the V and GV groups, the microbes were not completely eradicated, which may be closely associated with the relatively higher doses of bacteria inoculation (1×10^6 CFUs/mL) in our *in vivo* assay as compared with the numbers clinically contaminating bacteria in a surgical site [6]. In addition, the HACC was coated over the surfaces of the absorbable sutures, which may

restrict the loading capacity of these antibacterial sutures. Furthermore, the drug eluting rate may be accelerated due to the inevitable digestion by collagenase under an *in vivo* environment. Therefore, the current study just proved the feasibility of an antimicrobial cation agent serving as the suture coating material, and future studies need to be followed to improve the loading efficiency, as well as releasing time of HACC in the suture.

Conclusion

Both *in vitro* and *in vivo* studies demonstrated that the HACC-coated absorbable Vicryl sutures showed significant antibacterial potential (especially for drug-resistant strains) and good biocompatibility, which implies that such an antimicrobial agent-loaded suture may be an alternative option to prevent postoperative SSI in orthopaedic procedures.

Conflicts of interest

The authors declare no conflicts of interest in this work.

Funding/support

This research was financially supported by the National Key R and D Program (2016YFC1102100), the Shanghai Science and Technology Development Fund (13JC1403900), and the Medical Engineering Collaborative Project of Shanghai Jiao Tong University (YG2014ZD01).

References

[1] Fry DE. A system approach to the prevention of surgical infections. Surg Clin North Am 2009;89:521—37.
[2] Anderson DJ, Podgorny K, Berríos-Torres SI, Bratzler DW, Dellinger EP, Greene L, et al. Strategies to prevent surgical site infections in acute care hospitals: 2014 update. Infect Control Hosp Epidemiol 2014;35(Suppl. 2):S66—88.
[3] Jones RS, Brown C, Opelka F. Surgeon compensation: "Pay for performance," the American College of Surgeons National Surgical Quality Improvement Program, the Surgical Care Improvement Program, and other considerations. Surgery 2005;138:829—36.
[4] Richards G, Morgenstern M, Metsemakers WJ, Schwarz E, Awad H. AO Trauma clinical priority program bone infection. J Orthop Trans 2016;7:45.
[5] Lee KJ, Goodman SB. Indentification of periprosthetic joint infection after total hip arthroplasty. J Orthop Trans 2015;3:21—5.
[6] Edmiston Jr CE, Krepel CJ, Marks RM, Rossi PJ, Sanger J, Goldblatt M, et al. Microbiology of explanted suture segments from infected and noninfected surgical patients. J Clin Microbiol 2013;51:417—21.
[7] Justinger C, Slotta JE, Ningel S, Gräber S, Kollmar O, Schilling MK. Surgical-site infection after abdominal wall closure with triclosan-impregnated polydioxanone sutures: Results of a randomized clinical pathway facilitated trial (NCT00998907). Surgery 2013;154:589—95.
[8] Justinger C, Moussavian MR, Schlueter C, Kopp B, Kollmar O, Schilling MK. Antibiotic coating of abdominal closure sutures and wound infection. Surgery 2009;145:330—4.
[9] Fleck T, Moidl R, Blacky A, Fleck M, Wolner E, Grabenwoger M, et al. Triclosan-coated sutures for the reduction of sternal wound infections: economic considerations. Ann Thorac Surg 2007;84:232—6.
[10] Edmiston Jr CE, Daoud FC, Leaper D. Is there an evidence-based argument for embracing an antimicrobial (triclosan)-coated suture technology to reduce the risk for surgical-site infections? A meta-analysis. Surgery 2013;154:89—100.
[11] Daoud FC, Edmiston Jr CE, Leaper D. Meta-analysis of prevention of surgical site infections following incision closure with triclosan-coated sutures: robustness to new evidence. Surg Infect 2014;15:165—81.
[12] Ming X, Nichols M, Rothenburger S. In vivo antibacterial efficacy of MONOCRYL plus antibacterial suture (Poliglecaprone 25 with triclosan). Surg Infect 2007;8:209—14.
[13] Ming X, Rothenburger S, Nichols MM. In vivo and in vitro antibacterial efficacy of PDS plus (polidioxanone with triclosan) suture. Surg Infect 2008;9:451—7.
[14] Wang X, Chen X, Feng X, Chang F, Chen M, Xia Y, et al. Triclosan causes spontaneous abortion accompanied by decline of estrogen sulfotransferase activity in humans and mice. Sci Rep 2015;5:18252.
[15] Han J, Won EJ, Hwang UK, Kim IC, Yim JH, Lee JS. Triclosan (TCS) and Triclocarban (TCC) cause lifespan reduction and reproductive impairment through oxidative stress-mediated expression of the defensome in the monogonont rotifer (Brachionus koreanus). Comp Biochem Physiol C Toxicol Pharmacol 2016;185—186:131—7.
[16] Syed AK, Ghosh S, Love NG, Boles BR. Triclosan promotes Staphylococcus aureus nasal colonization. MBio 2014;5:e01015.
[17] Cao G, Sun Y, Chen J, Song L, Jiang J, Liu Z, et al. Sutures modified by silver-loaded montmorillonite with antibacterial properties. Appl Clay Sci 2014;93—94:102—6.
[18] Blaker JJ, Nazhat SN, Boccaccini AR. Development and characterisation of silver-doped bioactive glass coated sutures for tissue engineering and wound healing applications. Biomaterials 2004;25:1319—29.
[19] Serrano C, García-Fernández L, Fernández-Blázgue JP, Barbeck M, Ghanaati S, Unger R, et al. Nanostructured medical sutures with antibacterial properties. Biomaterials 2015;52:291—300.
[20] Peng Z, Wang L, Du L, Guo S, Wang X, Tang T. Adjustment of the antibacterial activity and biocompatibility of hydroxypropyltrimethyl ammonium chloride chitosan by varying the degree of substitution of quaternary ammonium. Carbohydr Polym 2010;81:275—83.
[21] Tan H, Ao H, Ma R, Tang T. Quaternised chitosan-loaded polymethylmethacrylate bone cement: biomechanical and histological evaluations. J Orthop Trans 2013;1:57—66.
[22] Tan H, Peng Z, Li Q, Xu X, Guo S, Tang T. The use of quaternised chitosan-loaded PMMA to inhibit biofilm formation and downregulate the virulence-associated gene expression of antibiotic-resistant staphylococcus. Biomaterials 2012;33:365—77.
[23] Peng Z, Tu B, Shen Y, Du L, Wang L, Guo S, et al. Quaternized chitosan inhibits *ica*A transcription and biofilm formation by Staphylococcus on a titanium surface. Antimicrob Agents Chemother 2011;55:860—6.
[24] Tan H, Ao H, Ma R, Lin W, Tang T. In vivo effect of quaternized chitosan-loaded polymethylmethacrylate bone cement on Methicillin-resistant Staphylococcus epidermidis infection of the tibial metaphysis in a rabbit model. Antimicrob Agents Chemother 2014;58:6016—23.
[25] Marcotte L, Barbeau J, Lafleur M. Permeability and thermodynamics study of quaternary ammonium surfactants-phosphocholine vesicle system. J Colloid Interface Sci 2005;292:219—27.

[26] Crismaru M, Asri LA, Loontjens TJ, Krom BP, de Vries J, van der Mei HC. Survival of adhering Staphylococci during exposure to a quaternary ammonium compound evaluated by using atomic force microscopy imaging. Antimicrob Agents Chemother 2011;55:5010—7.
[27] Mazzocca AD, McCarthy MB, Arciero C, Jhaveri A, Obopilwe E, Rincon L, et al. Tendon and bone responses to a collagen-coated suture material. J Shoulder Elbow Surg 2007;16:S222—30.
[28] Lin WT, Tan H, Duan ZL, Yue B, Ma R, He G, et al. Inhibited bacterial biofilm formation and improved osteogenic activity on gentamicin-loaded titania nanotubes with various diameters. Int J Nanomedicine 2014;9:1215—30.
[29] Lin WT, Zhang YY, Tan HL, Ao HY, Duan ZL, He G, et al. Inhibited bacterial adhesion and biofilm formation on quaternized chitosan-loaded titania nanotubes with various diameters. Materials 2016;9:155.
[30] Frutos Cabanillas P, Diez Pena E, Barrales-Rienda JM, Frutos G. Validation and in vitro characterization of antibiotic-loaded bone cement release. Int J Pharm 2000;209:15—26.
[31] Laurentin A, Edwards CA. A microtiter modification of the anthrone-sulfuric acid colorimetric assay for glucose-based carbohydrates. Anal Biochem 2003;315:143—5.
[32] Cole AM, Weis P, Diamond G. Isolation and characterization of pleurocidin, an antimicrobial peptide in the skin secretions of winter flounder. J Biol Chem 1997;272:12008—13.
[33] Zhang S, Liu X, Wang H, Peng J, Wong KK. Silver nanoparticle-coated suture effectively reduces inflammation and improves mechanical strength at intestinal anastomosis in mice. J Pediatr Surg 2014;49:606—13.
[34] van de Belt H, Neut D, Schenk W, van Horn JR, van der Mei HC, Busscher HJ. Staphylococcus aureus biofilm formation on different gentamicin-loaded polymethylmethacrylate bone cements. Biomaterials 2001;22:1607—11.
[35] Mathur T, Singhal S, Khan S, Upadhyay D, Fatma T, Rattan A. Detection of biofilm formation among the clinical isolates of staphylococci: an evaluation of three different screening methods. Indian J Med Microbiol 2006;24:25—9.
[36] Brembilla NC, Dufour AM, Alvarez M, Huques S, Montanari E, Truchetet ME, et al. IL-22 capacitates dermal fibroblast responses to TNF in scleroderma. Ann Rheum Dis 2016;75:1697—705.
[37] Ma R, Tang S, Tan H, Lin W, Wang Y, Wei J, et al. Preparation, characterization, and in vitro osteoblast functions of a nano-hydroxyapatite/polyetheretherketone biocomposite as orthopedic implant material. Int J Nanomedicine 2014;9:3949—61.
[38] Fang SJ, Meng XD, Zhang ZH, Wang Y, Liu YY, You CY, et al. Vorinostat modulates the imbalance of T cell subsets, suppresses macrophage activity, and ameliorates experimental autoimmune uveoretinitis. Neuromol Med 2016;18:134—45.
[39] Varma S, Ferguson HC, Breen DV, Lumb WV. Comparison of seven suture materials in infected wounds: an experimental study. J Surg Res 1974;17:165—70.
[40] Ridgeway S, Wilson J, Charlet A, Kafatos G, Pearson A, Coello R. Infection of the surgical site after arthroplasty of the hip. J Bone Joint Surg Br 2005;87:844—50.
[41] Edward C, Counsell A, Boulton C, Moran CG. Early infection after hip fracture surgery: risk factors, costs and outcome. J Bone Joint Surg Br 2008;90:770—7.
[42] Xu SG, Mao ZG, Liu BS, Zhu HH, Pan HL. Evaluating the use of antibiotic prophylaxis during open reduction and internal fixation surgery in patients at low risk of surgical site infection. Injury 2015;46:184—8.
[43] Gristina AG, Hobgood CD, Webb LX, Myrvik QN. Adhesive colonization of biomaterials and antibiotic resistance. Biomaterials 1987;8:423—6.
[44] Donlan RM, Costerton JW. Biofilms: survival mechanisms of clinically relevant microorganisms. J Clin Microbiol Rev 2002;15:167—93.